

# Position Control of Active Magnetic Bearing (AMB) Using Luenberger-like Observer Based Backstepping Control

Jihad S. Radaideh\*

Mechanical Engineering Department, Al-Huson University College, Al-Balqa Applied University, P.O.B (50), 21510 Al-Huson -Jordan

Received 26 Jun 2023

Accepted 22 Jul 2023

## Abstract

In this paper, an observer based back-stepping control (BS) is developed to regulate the position of the rotor shaft in an Active Magnetic Bearing (AMB). A large deviation of the rotor from its equilibrium position can cause serious failure of operation. The objective is to control the deviation of the magnetic bearing from its nominal position in the presence of disturbances. The backstepping control formulation results in a state equation with Skew-Symmetric Hurwitz linear system matrix. This form of equation is of great importance and can be utilized for many analysis and control purposes. For this equation, a Luenberger-like observer is designed to estimate the states of the system, and then the estimated states are used in the controller, adding more stability and robustness. Simulation results proved excellent performance of the observer-based BS controller and its robustness to disturbances.

© 2023 Jordan Journal of Mechanical and Industrial Engineering. All rights reserved

**Keywords:** Backstepping control; Active Magnetic Bearing; Luenberger observer; Lyapunov.

## 1. Introduction

There are two kinds of magnetic bearing: passive and active. A passive magnetic bearing is made of permanent magnets, so the output flux cannot be adjusted while an active magnetic bearing (AMB) is made of electromagnets and the output flux can be adjusted by changing the current on the coil. The magnetic force in the AMB can be controlled to achieve rotor stable operation with vibration control so that there is no friction between the rotor and the bearing. The dynamic adjustable characteristics of the AMB which can achieve active control of rotor shaft position and vibration reduction made it much more popular than passive magnetic bearing. The use of AMB in high-speed rotation machines has recently increased, even though it is mostly popular in stationary applications, it was proved recently that the system is capable in motion-based applications such as submarine propulsion systems, jet engines and hybrid electric vehicles [1]. AMB has been widely used in compressors in industrial applications because of their high performance and reliability for more than 2 decades. The capability of the AMB to keep the rotor near the clearance center during operation enables compressors to operate efficiently at high rotational speeds [2].

The AMB suspends a rotor in a magnetic field, the rotor spins at a high speed, because of its high-speed rotation and a small air gap between the rotor and stator, a large deviation of rotor from its equilibrium position may cause failure of the operation. Therefore, we need to control the position of the rotor to maintain stable operations.

Many published papers investigate different control approaches. The well-known and popular Proportional-Integral-Derivative Control (PID) is investigated [3] and [4] and [5]. In [3] a cascaded PI/PD approach is proposed with current and position feedback signals. Although PID is easy to implement, it is not robust to disturbances and uncertainties caused by inaccuracies in system parameters and

unmodeled dynamics if not combined with other methods. An improved PID design can be found in [6]. In [7] and [8], PID, PI/PD genetic algorithm (GA) and LQR are compared. In [9], an optimal PD controller is implemented. In [10] a Linear Quadratic Regulator (LQR) was designed and implemented. Other sensorless control methods are proposed in [11] and [1] where the sensors are eliminated, and the position is determined by other methods such as coil currents. An estimator was developed in [12] to estimate the length of the bearing airgap while rejecting the influence of amplifier voltage and duty-cycle variation. In [13], a dynamic modeling method for AMB system considering both translational and rotational base motions was investigated. In [14], a sliding mode controller was implemented to a reduced order model of the AMB. Fuzzy controllers were investigated in [15]. An efficient self-tuning fuzzy controller was developed in [16]. An iterative learning control to deal with periodic vibration problem caused by unbalanced force existing in AMB was developed in [17]. Convolutional neural networks were investigated in [18]. A state-constraints adaptive backstepping control strategy is developed in [19] to accomplish precise rotor displacement control for a nonlinear AMB system. [20] presents a disturbance suppression by using a nonlinear disturbance observer and an extended state observer for a nonlinear active magnetic bearing system and then a fuzzy sliding mode controller is applied for rotor displacement control. In [21], an extended state observer based field dynamic balancing strategy for rotating machinery equipped with AMB is proposed. The observer is designed according to open loop dynamics of the system which makes it irrelevant with the closed loop control algorithm design. In [2], a fractional-order proportional-derivative control that results in the required specifications of surge control with a simple controller structure was implemented on a centrifugal compressor equipped with AMBs. Adaptive MIMO pole placement was investigated in [22]. In [23], a disturbance rejection with controllers based on Lur'e system approach is implemented. The nonlinear magnetization was modeled

\* Corresponding author e-mail: radaidehjehad@yahoo.com.

as a Lur'e system and LMIs for stability in the performance of the closed-loop system.

Observers are used to estimate the system's unmeasurable states or states that are expensive to measure. It also removes noise from sensor measurements to add more stability to the control system. Knowledge of the system state is significantly important to solve many control problems such as state feedback. In this paper, observer-based backstepping control is developed to regulate the position of the rotor shaft in the AMB system. Backstepping control is a recursive Lyapunov-based design technique known for its tracking and regulation capabilities and robustness to disturbances [24] and [25]. It can be considered as a special case of the known feedback linearization, where we stabilize the system using the state variables. Unlike the feedback linearization which cancels all the nonlinear terms in the state equation, the backstepping does not necessarily cancel all the nonlinearities, which gives us the freedom to keep some useful nonlinearities that can be used to add damping to further stabilize the dynamical system. The design procedure of the backstepping consists of designing a series of control laws recursively by using the state variables in the system as virtual controls and replacing them with stabilizing functions. Since there will always be an error between the state variables and their stabilizing functions, a new state equation or a new coordinate system is introduced, called the error domain or the  $z$ -domain. The new state equation results in a skew symmetric system matrix. This form of matrix is very important in control theory because it is always Hurwitz (stable) and linear. Linear control and observer methods can be designed for this state equation such as, pole placement, linear quadratic regulator (LQR), and Luenberger observer since linear control and observer methods are considerably easier to understand and analyze than nonlinear methods, and then after applying these linear control methods to the system in the new coordinate system ( $z$ -domain), it can be converted back to the original form, which we call the  $x$ -domain.

This paper has two contributions. The first one is the design of a Luenberger-like observer in the error domain or the  $z$ -domain and then converting it to the  $x$ -domain. With this method, the stability and convergence of the estimated states to the true states is proved. The observer is applied to the Skew-Symmetric Hurwitz matrix that results from the backstepping control formulation. Because this matrix is Skew-Symmetric and Skew-Symmetric matrices are always stable, the stability and convergence of the of the designed observer is also guaranteed. The previous methods done in designing a state observer for an AMB were based on the original system which is originally unstable with no transformation. The second contribution is the derivation of the observer based backstepping controller to regulate the position of the rotor shaft.

The paper is organized as follows; the system model is discussed in section 2. The backstepping controller is derived in section 3 in the new coordinate system ( $z$ -domain) and converted back to the original coordinate system ( $x$ -domain) in section 4. The Luenberger-like observer is designed in section 5 based on the Skew-Symmetric Hurwitz matrix derived in section 3. The observer is converted from the  $z$ -domain to the  $x$ -domain in section 6. Simulation results are discussed in section 7 and the method's limitations are discussed in section 8, and finally the conclusion and future work are discussed in section 9.

## 2. System Model

The figure (1) shows the system model for an AMB system [26]. The parameters configuration in Table 1 are also taken from [26].

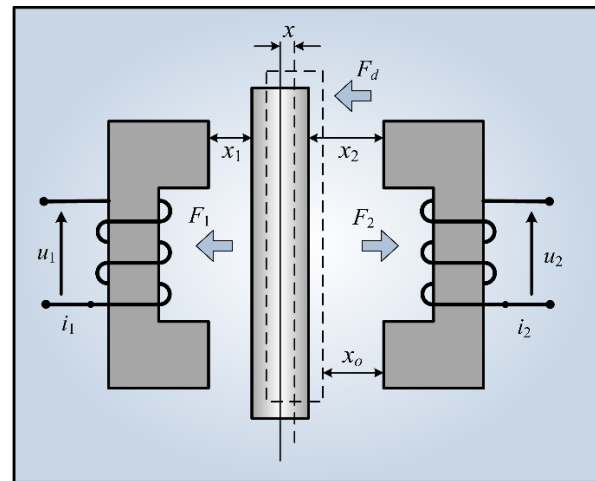


Figure 1. AMB circuit diagram

Where  $i_1$  and  $i_2$  are coil 1 and coil 2 currents respectively,  $F_1$  and  $F_2$  are the opposite electromagnetic forces generated by currents 1 and 2 respectively,  $u_1$  and  $u_2$  are the input voltage,  $x$  is the displacement of the rotor from nominal position  $x_0$ .  $x_1$  and  $x_2$  are the air gaps between the left and right stators respectively,  $F_d$  is the disturbance. The rotor in the middle of the two cores rotates in a plain perpendicularly to the figure. The input voltage  $u_1$  and  $u_2$  can be adjusted to control the two currents  $i_1$  and  $i_2$  in order to determine the resultant force.

The nonlinear system model of the AMB is given by [26] and [27] as shown below,

$$\left. \begin{aligned} \dot{x} &= v \\ \dot{v} &= \frac{k}{4m} \left( \frac{i_1}{x_0-x} \right)^2 - \frac{k}{4m} \left( \frac{i_2}{x_0+x} \right)^2 + \frac{F_d}{m} \\ i_1 &= \frac{2(x_0-x)}{2L_s(x_0-x)+k} \left[ -Ri_1 - \frac{k}{2(x_0-x)^2} v i_1 + u_1 \right] \\ i_2 &= \frac{2(x_0+x)}{2L_s(x_0+x)+k} \left[ -Ri_2 + \frac{k}{2(x_0+x)^2} v i_2 + u_2 \right] \end{aligned} \right\} \quad (1)$$

Which can be rewritten as,

$$\left. \begin{aligned} \dot{x}_1 &= x_2 \\ \dot{x}_2 &= \frac{k}{4m} \left( \frac{x_3}{x_0-x_1} \right)^2 - \frac{k}{4m} \left( \frac{x_4}{x_0+x_1} \right)^2 + \frac{F_d}{m} \\ \dot{x}_3 &= \frac{2(x_0-x_1)}{2L_s(x_0-x_1)+k} \left[ -R x_3 - \frac{k}{2(x_0-x_1)^2} x_2 x_3 + u_1 \right] \\ \dot{x}_4 &= \frac{2(x_0+x_1)}{2L_s(x_0+x_1)+k} \left[ -R x_4 + \frac{k}{2(x_0+x_1)^2} x_2 x_4 + u_2 \right] \end{aligned} \right\} \quad (2)$$

Table 1. Parameter Configuration

Symbol	Quantity	Value (unit)
$K_s$	Force-Displacement Constant	142860 N/m
$K_i$	Force-Current constant	100 N/A
$L_s$	Coil Self Inductance	120 mH
$L_o$	Air Gap Inductance	70 mH
$m$	Weight of Rotor	4.6 kg
$R$	Coil Resistance	8 $\Omega$
$x_0$	Nominal Air Gap	1 mm
$i_0$	Bias current	1 A
$F_d$	Disturbance Force	4.6 N

## 3. Backstepping Controller Design

Jacobian linearization technique is used to linearize the system before the backstepping control design to simplify the control development. Details of linearization can be found in [27]. A

comparative study of Jacobian linearization method with optimal linear model can be found in [28].

The resulting linear system

$$\begin{bmatrix} \dot{x}_1 \\ \dot{x}_2 \\ \dot{x}_3 \\ \dot{x}_4 \end{bmatrix} = \begin{bmatrix} 0 & 1 & 0 & 0 \\ \frac{2k_s}{m} & 0 & \frac{k_i}{m} & -\frac{k_i}{m} \\ 0 & -\frac{k_i}{L} & -\frac{R}{L} & 0 \\ 0 & \frac{k_i}{L} & 0 & -\frac{R}{L} \end{bmatrix} \begin{bmatrix} x_1 \\ x_2 \\ x_3 \\ x_4 \end{bmatrix} + \begin{bmatrix} 0 & 0 \\ 0 & 0 \\ \frac{1}{L} & 0 \\ 0 & \frac{1}{L} \end{bmatrix} \begin{bmatrix} u_1 \\ u_2 \end{bmatrix} + \begin{bmatrix} 0 \\ \frac{1}{m} \\ 0 \\ 0 \end{bmatrix} F_d$$

where as in [27],

$$k_s = \frac{k_i^2}{2x_0^3}, k_i = \frac{k_i^2}{2x_0^2}, L = \frac{k+2x_0L_s}{2x_0}$$

The above fourth-order MIMO system was transformed into a third-order SISO subsystem and a first-order SISO subsystem by change of variables and the details can be found in [27].

For the resulting third-order SISO subsystem, we are going to design a backstepping control and a backstepping-based observer. The third-order SISO subsystem is given by,

$$\begin{bmatrix} \dot{x}_1 \\ \dot{x}_2 \\ \dot{x}_3 \end{bmatrix} = \begin{bmatrix} 0 & 1 & 0 \\ \frac{2k_s}{m} & 0 & \frac{2k_i}{m} \\ 0 & -\frac{k_i}{L} & -\frac{R}{L} \end{bmatrix} \begin{bmatrix} x_1 \\ x_2 \\ x_3 \end{bmatrix} + \begin{bmatrix} 0 \\ 0 \\ \frac{1}{L} \end{bmatrix} u + \begin{bmatrix} 0 \\ \frac{1}{m} \\ 0 \end{bmatrix} F_d, y = x_1.$$

Or can be written as

$$\begin{bmatrix} \dot{x} \\ \dot{v} \\ \dot{i} \end{bmatrix} = \underbrace{\begin{bmatrix} 0 & 1 & 0 \\ a & 0 & b \\ 0 & c & d \end{bmatrix}}_A \begin{bmatrix} x \\ v \\ i \end{bmatrix} + \underbrace{\begin{bmatrix} 0 \\ 0 \\ e \end{bmatrix}}_B u + \underbrace{\begin{bmatrix} 0 \\ f \\ 0 \end{bmatrix}}_{B_d} F_s, \quad (3)$$

$$y = x_1.$$

Where  $x$  is the displacement of rotor from nominal position,  $v$  is velocity, and  $i$  is the current.

$$a = \frac{2k_s}{m}, b = \frac{2k_i}{m}, c = \frac{k_i}{L_0+L_s}, d = \frac{-R}{L_0+L_s}, e = \frac{1}{L_0+L_s}, f = \frac{1}{m}$$

From the above linear system, the eigenvalues of the system matrix  $A$  were computed using MATLAB, one of them was positive which implies that the system is unstable, but the pair  $[A, B]$  is controllable, so we can design a controller to stabilize the system. The design procedure of the system was developed with some reference to [29] and [30], which applies the backstepping method to electric power steering control and trajectory tracking control.

The state equations of the AMB can be transformed to the “strict feedback form” for the design of the backstepping controller.

The strict feedback form of the system is given by,

$$\dot{x} = f(x) + g(x)u$$

$$\begin{bmatrix} \dot{x}_1 \\ \dot{x}_2 \\ \dot{x}_3 \end{bmatrix} = \begin{bmatrix} x_2 \\ \frac{a}{b}x_1 + x_3 + \theta \\ cbx_2 + dx_3 \end{bmatrix} + \begin{bmatrix} 0 \\ 0 \\ e \end{bmatrix} u. \quad (4)$$

where

$$x_1 = \frac{1}{b}x, x_2 = \frac{1}{b}v, x_3 = i, \theta = \frac{F_s}{bm}, \dot{u} = \frac{1}{e}u.$$

The control objective is to stabilize the AMB and to drive the position of the rotor shaft to its equilibrium point so that it remains mid-way between the two coils in the presence of an external disturbance force.

Note: in [26] adaptive backstepping is applied to estimate the disturbance, but in this paper, we are going to assume that the disturbance is known, so backstepping is applied without adaptive laws. Also in this paper, the parameters of the system are assumed known, so there are no adaptive laws to estimate the system’s

parameters. A complete systematic way of designing adaptive laws for parameter estimation is discussed in [31].

**Step 1:** stabilizing subsystem  $\dot{x}_1 = x_2$  using the stabilizing function  $\alpha_1$ .

Treating  $x_2$  as the virtual control of the subsystem  $\dot{x}_1 = x_2$ , the first step is to find its stabilizing function  $\alpha_1$ . We define the error variables as,

$$z_1 = x_1, \quad (5)$$

$$z_2 = x_2 - \alpha_1, \quad (6)$$

Taking the derivative of  $z_1$  yields

$$\dot{z}_1 = \dot{x}_1 = x_2 = z_2 + \alpha_1. \quad (7)$$

The Lyapunov function to stabilize the first error  $z_1$  is.

$$V_1 = \frac{1}{2}z_1^2, \quad (8)$$

$$\dot{V}_1 = z_1\dot{z}_1 = z_1(z_2 + \alpha_1) = z_1z_2 + z_1\alpha_1. \quad (9)$$

Choosing  $\alpha_1 = -c_1z_1$  and assuming  $z_2 = 0$ , as will be seen later, guarantees Eq. (9) is negative definite.

Substituting  $\alpha_1$  in Eqs. (7) and (9) yields,

$$\dot{z}_1 = z_2 + \alpha_1 = z_2 - c_1z_1, \quad (10)$$

$$\dot{V}_1 = z_1z_2 - c_1z_1^2, \quad c_1 > 0. \quad (11)$$

**Step 2:** stabilizing subsystem  $(\dot{x}_2 = \frac{a}{b}x_1 + x_3 + \theta)$  using the stabilizing function  $\alpha_2$ .

Treating  $x_3$  as the virtual control, we need to determine its stabilizing function  $\alpha_2$ .

The third error variable is defined as,

$$z_3 = x_3 - \alpha_2, \quad (12)$$

To proceed, we need to find the derivative of the second error variable ( $z_2 = x_2 - \alpha_1$ ),

$$\begin{aligned} \dot{z}_2 &= \dot{x}_2 - \dot{\alpha}_1 = \frac{a}{b}x_1 + x_3 + \theta - \dot{\alpha}_1 \\ &= \frac{a}{b}x_1 + \theta + z_3 + \alpha_2 - \dot{\alpha}_1. \end{aligned} \quad (13)$$

In this step we are going to stabilize the  $(z_1, z_2)$  error system given by Eqs. (10) and (13). The Lyapunov function is chosen as,

$$V_2 = V_1 + \frac{1}{2}z_2^2, \quad (14)$$

$$\begin{aligned} \dot{V}_2 &= \dot{V}_1 + z_2\dot{z}_2 \\ &= -c_1z_1^2 + z_2z_3 + z_2(z_1 + \alpha_2 + \frac{a}{b}x_1 + \theta - \dot{\alpha}_1), \\ c_1 &> 0, \quad c_2 > \end{aligned} \quad (15)$$

Assuming  $z_3 = 0$ , as will be shown in the next step, and choosing  $\alpha_2$  to make the term  $z_1 + \alpha_2 + \frac{a}{b}x_1 + \theta - \dot{\alpha}_1 = -c_2z_2$  in Eq. (15) yields,

$$\alpha_2 = -z_1 - c_2z_2 + \dot{\alpha}_1 - \frac{a}{b}x_1 - \theta, \quad (16)$$

Substituting Eq. (16) in Eq. (13) yields,

$$\dot{z}_2 = -z_1 - c_2z_2 + z_3, \quad (17)$$

Substituting Eq. (16) in Eq. (15) yields,

$$\dot{V}_2 = z_2z_3 - c_1z_1^2 - c_2z_2^2. \quad (18)$$

**Step 3:** Stabilizing the complete system using the backstepping control law  $u$ .

Taking the derivative of  $z_3$  yields,

$$\dot{z}_3 = \dot{x}_3 - \dot{\alpha}_2 = cbx_2 + dx_3 + \dot{u} - \dot{\alpha}_2, \quad (19)$$

The Lyapunov function  $V_3$  is chosen as,

$$V_3 = V_2 + \frac{1}{2}z_3^2, \tag{20}$$

$$\dot{V}_3 = -c_1z_1^2 - c_2z_2^2 + z_3(z_2 + cbx_2 + dx_3 + \dot{u} - \dot{\alpha}_2), \tag{21}$$

We choose  $u$  as,

$$\dot{u} = -z_2 - c_3z_3 - cbx_2 - dx_3 + \dot{\alpha}_2, \tag{22}$$

Substituting Eq. (22) in Eq. (19) yields,

$$\dot{z}_3 = -z_2 - c_3z_3, \tag{23}$$

Substituting Eq. (22) in Eq. (21) yields,

$$\dot{V}_3 = -c_1z_1^2 - c_2z_2^2 - c_3z_3^2, \quad c_1 > 0, c_2 > 0, c_3 > 0.$$

$\dot{V}_3$  is negative definite guarantying  $z_1, z_2$  and  $z_3$  goes to zero as time goes to infinity and the system is globally uniformly asymptotically stable by Lasalle-Yoshizawa Theorem taken from [24].

### 3.1. Lasalle-Yoshizawa Theorem [24]

Let  $x = 0$  be an equilibrium point of  $\dot{x} = f(x, t)$  and suppose  $f$  is locally Lipschitz in  $x$  uniformly in  $t$ . Let  $V: R^n \rightarrow R_+$  be a continuously differentiable function such that

$$\dot{V} = \frac{\partial V}{\partial x}(x)f(x, t) \leq -W(x) \leq 0, \forall t \geq 0, \forall x \in R^n$$

Where  $W$  is a continuous function. Then all solutions of  $\dot{x} = f(x, t)$  are globally uniformly bounded and satisfy  $\lim_{t \rightarrow \infty} |x(t)| = 0$ . In addition, if  $W(x)$  is positive definite then the equilibrium  $x = 0$  is globally uniformly asymptotically stable GUAS.

The complete error system given by Eqs. (10), (17) and (23) can be expressed as,

$$\begin{bmatrix} \dot{z}_1 \\ \dot{z}_2 \\ \dot{z}_3 \end{bmatrix} = \begin{bmatrix} -c_1 & 1 & 0 \\ -1 & -c_2 & 1 \\ 0 & -1 & -c_3 \end{bmatrix} \begin{bmatrix} z_1 \\ z_2 \\ z_3 \end{bmatrix}. \tag{24}$$

Since the above skew symmetric Hurwitz matrix is linear, we can design a Luenberger-like observer for the system in the  $z$ -domain and then convert it to the  $x$ -domain which is done later in this paper.

### 4. Converting the System from the z-Domain to the x-Domain

We obtain from Eq. (24) with Eqs. (7), (13) and (19)

$$\begin{bmatrix} \dot{x}_1 \\ \dot{x}_2 \\ \dot{x}_3 \end{bmatrix} = \begin{bmatrix} x_2 \\ \frac{a}{b}x_1 + x_3 + \theta \\ cbx_2 + dx_3 \end{bmatrix} + \begin{bmatrix} 0 \\ 0 \\ 1 \end{bmatrix} \dot{u}, \tag{25}$$

$$\begin{aligned} \dot{u} &= -z_2 - c_3z_3 - cbx_2 - dx_3 + \dot{\alpha}_2, \\ \alpha_1 &= -c_1z_1 = -c_1x_1, \quad \dot{\alpha}_1 = -c_1\dot{z}_1 = -c_1x_2, \end{aligned}$$

$$\alpha_2 = -\left(1 + c_1c_2 + \frac{a}{b}\right)x_1 - (c_1 + c_2)x_2 - \theta, \tag{26}$$

$$\begin{aligned} \dot{\alpha}_2 &= -\left(1 + c_1c_2 + \frac{a}{b}\right)x_2 - (c_1 + c_2)x_3 \\ &\quad - \frac{a}{b}(c_1 + c_2)x_1 - (c_1 + c_2)\theta - \dot{\theta}. \end{aligned} \tag{27}$$

$$\begin{aligned} z_2 &= x_2 - \alpha_1. \\ z_3 &= x_3 - \alpha_2. \end{aligned}$$

Substituting Eqs. (6), (12) and (27) in Eq. (22) yield,

$$\begin{aligned} \dot{u} &= -\left(c_1 + c_3 + c_1c_2c_3 + \frac{a}{b}(c_1 + c_2 + c_3)\right)x_1 \\ &\quad - \left(c_1c_2 + c_1c_3 + c_2c_3 + 2 + cb + \frac{a}{b}\right) \\ &\quad - (c_1 + c_2 + c_3 + d)x_3 - (c_1 + c_2 + c_3)\theta - \dot{\theta}, \end{aligned} \tag{28}$$

Substituting Eq. (28) in Eq. (25) the term  $(-cbx_2 - dx_3)$  in Eq. (28) cancels the term  $(cbx_2 + dx_3)$  in Eq. (25) which yields the closed loop system,

$$\begin{bmatrix} \dot{x}_1 \\ \dot{x}_2 \\ \dot{x}_3 \end{bmatrix} = \begin{bmatrix} 0 & 1 & 0 \\ \frac{a}{b} & 0 & 1 \\ a_{31} & a_{32} & a_{33} \end{bmatrix} \begin{bmatrix} x_1 \\ x_2 \\ x_3 \end{bmatrix} = \begin{bmatrix} 0 & 1 & 0 \\ \frac{a}{b} & 0 & 1 \\ a_{31} & a_{32} & a_{33} \end{bmatrix} \begin{bmatrix} x_1 \\ x_2 \\ x_3 \end{bmatrix} + \begin{bmatrix} 0 \\ \theta \\ -(c_1 + c_2 + c_3)\theta - \dot{\theta} \end{bmatrix}. \tag{29}$$

where

$$\begin{aligned} a_{31} &= \left(c_1 + c_3 + c_1c_2c_3 + \frac{a}{b}(c_1 + c_2 + c_3)\right) \\ a_{32} &= c_1c_2 + c_1c_3 + c_2c_3 + 2 + \frac{a}{b} \\ a_{33} &= c_1 + c_2 + c_3 \end{aligned}$$

### 5. Luenberger-Like Observer Design

In this section a Luenberger-like observer is designed based on the skew-symmetric form obtained in Eq. (24). The observer can be constructed as follows,

$$\begin{aligned} \dot{\hat{z}} &= A_{ss}\hat{z} + L_{bs}(\tilde{y} - C\hat{z}) \\ &= \underbrace{(A_{ss} - L_{bs}C)}_{A_{bs}}\hat{z} + L_{bs}\tilde{y}, \end{aligned} \tag{30}$$

$$\tilde{y} = Cz$$

where  $A_{ss} = \begin{bmatrix} -c_1 & 1 & 0 \\ -1 & -c_2 & 1 \\ 0 & -1 & -c_3 \end{bmatrix}$ .

$C = [1 \ 0 \ 0]$ ,  $[A_{ss}, C]$  is an observable pair,  
 $y = x_1, \tilde{y} = y - y_r = x_1 - y_r = z_1, \tilde{y} - C\hat{z} = y - \hat{x}_1$ .

$L_{bs} \in R^{3 \times 1}$  is the observer gain matrix to be obtained by pole placement such that  $A_{bs} = A_{ss} - L_{bs}C$  is Hurwitz and the real parts of  $A_{bs}$  are more negative than those of  $A_{ss}$ .

The estimation error  $\tilde{z} = z - \hat{z}$  satisfies,

$$\begin{aligned} \dot{\tilde{z}} &= \dot{z} - \dot{\hat{z}} = A_{ss}z - (A_{ss} - L_{bs}C)\hat{z} - L_{bs}\tilde{y} \\ &= (A_{ss} - L_{bs}C)(z - \hat{z}) = A_{bs}\tilde{z}. \end{aligned} \tag{31}$$

Since  $A_{ss}$  is Hurwitz, it follows that,

$$\lim_{t \rightarrow \infty} [\tilde{z}(t)] = \lim_{t \rightarrow \infty} [z(t) - \hat{z}(t)] = 0, \quad \tilde{z}(0) \neq 0. \tag{32}$$

### 6. Converting the Observer-Based Control to the x-Domain

We have the following proposition for implementing the complete observer-based control system in the  $x$ -domain.

**Proposition:** The backstepping-based observer can be expressed in the  $x$ -domain as,

$$\dot{\hat{x}} = f(\hat{x}) + g(\hat{x})\hat{u} + O^{-1}_{bs}L_{bs}(y - \hat{x}_1). \tag{33}$$

Where  $\hat{u}$  is the controller obtained in the backstepping design and  $O_{bs}^{-1}$  is the inverse of the observability matrix  $O_{bs}$ .

$$\hat{u}_{bs} = -Kx - \beta = -k_1x_1 - k_2x_2 - k_3x_3 - \beta, \tag{34}$$

where

$$\begin{aligned} k_1 &= c_1 + c_3 + c_1c_2c_3 + \frac{a}{b}(c_1 + c_2 + c_3). \\ k_2 &= \left(c_1c_2 + c_1c_3 + c_2c_3 + \frac{a}{b} + 2 + cb\right). \\ k_3 &= (c_1 + c_2 + c_3 + d). \\ \beta &= (c_1 + c_2 + c_3)\theta + \dot{\theta}. \end{aligned}$$

#### Proof

Utilizing the change of variables or error variables equations obtained in the backstepping design, the coordinate transformation  $T_{bs}$  associated with the error vector  $z$  is given by,

$$z = \begin{bmatrix} z_1 \\ z_2 \\ z_3 \end{bmatrix} = \begin{bmatrix} x_1 \\ x_2 - \alpha_1 \\ x_3 - \alpha_2 \end{bmatrix} = \begin{bmatrix} x_1 \\ c_1 x_1 + x_2 \\ a_1 \end{bmatrix} = T_{bs}(x, \theta). \quad (35)$$

where

$$\begin{aligned} \alpha_1 &= x_3 + \left(c_1 c_2 + \frac{a}{b} + 1\right) x_1 + (c_1 + c_2) x_2 + \theta. \\ \hat{\alpha}_1 &= -c_1 \hat{z}_1 = -c_1 \hat{x}_1. \end{aligned}$$

Utilizing

$$\hat{\alpha}_2 = -\left(1 + c_1 c_2 + \frac{a}{b}\right) \hat{x}_1 - (c_1 + c_2) \hat{x}_2 - \theta$$

yield,

$$\dot{z} = \begin{bmatrix} \dot{z}_1 \\ \dot{z}_2 \\ \dot{z}_3 \end{bmatrix} = \begin{bmatrix} \dot{x}_1 \\ \dot{x}_2 - \dot{\alpha}_1 \\ \dot{x}_3 - \dot{\alpha}_2 \end{bmatrix} = \begin{bmatrix} \dot{x}_1 \\ c_1 \dot{x}_1 + \dot{x}_2 \\ \dot{a}_1 \end{bmatrix} = T_{bs}(\dot{x}, \theta), \quad (36)$$

where

$$\dot{a}_1 = \dot{x}_3 + \left(c_1 c_2 + \frac{a}{b} + 1\right) \dot{x}_1 + (c_1 + c_2) \dot{x}_2 + \theta$$

Taking the derivative of the above equation yield,

$$\begin{aligned} \dot{z} &= \left(\frac{\partial T_{bs}}{\partial \dot{x}}\right) \dot{x} + \frac{\partial T_{bs}}{\partial \theta} \dot{\theta}. \quad (37) \\ O_{bs} &= \frac{\partial T_{bs}}{\partial \dot{x}} = \begin{bmatrix} 1 & 0 & 0 \\ c_1 & 1 & 0 \\ \left(c_1 c_2 + \frac{a}{b} + 1\right) & (c_1 + c_2) & 1 \end{bmatrix}, \quad (38) \end{aligned}$$

$$O_{bs}^{-1} = \begin{bmatrix} 1 & 0 & 0 \\ -c_1 & 1 & 0 \\ \left(c_1^2 - \frac{a}{b} - 1\right) & -(c_1 + c_2) & 1 \end{bmatrix}, \quad (39)$$

$$\frac{\partial T_{bs}}{\partial \theta} = \begin{bmatrix} 0 \\ 0 \\ 1 \end{bmatrix}. \quad (40)$$

where  $O_{bs}$  is called the **observability matrix** associated with the coordinate transformation  $z = T_{bs}(x, \theta)$ .

We obtain from Eqs. (30) and (37),

$$\begin{aligned} \dot{x} &= O_{bs}^{-1} \left[ \dot{z} - \frac{\partial T_{bs}}{\partial \theta} \dot{\theta} \right] \\ &= O_{bs}^{-1} \left[ A_{ss} \dot{z} + L_{bs} (\dot{y} - C \dot{z}) - \frac{\partial T_{bs}}{\partial \theta} \dot{\theta} \right] \\ &= O_{bs}^{-1} \left[ A_{ss} \dot{z} - \frac{\partial T_{bs}}{\partial \theta} \dot{\theta} \right] + O_{bs}^{-1} L_{bs} (\dot{y} - C \dot{z}) \\ &= O_{bs}^{-1} \left( \begin{bmatrix} -c_1 & 1 & 0 \\ -1 & -c_2 & 1 \\ 0 & -1 & -c_3 \end{bmatrix} \begin{bmatrix} \dot{z}_1 \\ \dot{z}_2 \\ \dot{z}_3 \end{bmatrix} - \begin{bmatrix} 0 \\ 0 \\ 1 \end{bmatrix} \dot{\theta} \right) \\ &+ O_{bs}^{-1} L_{bs} (\dot{y} - C \dot{z}) \\ &= O_{bs}^{-1} \begin{bmatrix} -c_1 \dot{z}_1 + \dot{z}_2 \\ -\dot{z}_1 - c_2 \dot{z}_2 + \dot{z}_3 \\ -\dot{z}_2 - c_3 \dot{z}_3 - \dot{\theta} \end{bmatrix} + O_{bs}^{-1} L_{bs} (\dot{y} - C \dot{z}) \\ &= O_{bs}^{-1} \begin{bmatrix} \underbrace{-c_1 \dot{z}_1 + \dot{z}_2}_{\dot{z}_1 = \dot{x}_2} \\ \underbrace{-\dot{z}_1 - c_2 \dot{z}_2 + \dot{z}_3}_{\dot{z}_2 = \dot{x}_3 + \frac{a}{b} \dot{x}_1 + \theta - \hat{\alpha}_1} \\ \underbrace{-\dot{z}_2 - c_3 \dot{z}_3 - \dot{\theta}}_{\dot{z}_3 = cb \dot{x}_2 + d \dot{x}_3 + \dot{u} - \hat{\alpha}_2} \end{bmatrix} + O_{bs}^{-1} L_{bs} (\dot{y} - C \dot{z}) \\ &= \begin{bmatrix} \dot{x}_2 \\ \dot{x}_3 + \frac{a}{b} \dot{x}_1 + \theta \\ \dot{u} + cb \dot{x}_2 + d \dot{x}_3 \end{bmatrix} + O_{bs}^{-1} L_{bs} (\dot{y} - C \dot{z}), \quad (41) \end{aligned}$$

Substituting Eq. (34) in Eq. (41), the term  $(-cb \dot{x}_2 - d \dot{x}_3)$  in  $\hat{u}_{bs}$  cancels the term  $(cb \dot{x}_2 + d \dot{x}_3)$  in Eq. (41) and it reduces to,

$$\begin{aligned} \dot{x} &= \begin{bmatrix} 0 & 1 & 0 \\ \frac{a}{b} & 0 & 1 \\ a_{obs31} & a_{obs32} & a_{obs33} \end{bmatrix} \begin{bmatrix} \hat{x}_1 \\ \hat{x}_2 \\ \hat{x}_3 \end{bmatrix} \\ &* \begin{bmatrix} 0 \\ \theta \\ -(c_1 + c_2 + c_3) \theta - \dot{\theta} \end{bmatrix} \\ &- \begin{bmatrix} L_{bs1} \\ -c_1 L_{bs1} + L_{bs2} \\ \left(c_1^2 - \frac{a}{b} - 1\right) L_{bs1} - (c_1 + c_2) L_{bs2} + L_{bs3} \end{bmatrix} \hat{x}_1 \\ &+ O_{bs}^{-1} L_{bs} y \\ &= \begin{bmatrix} \frac{a}{b} + c_1 L_{bs1} - L_{bs2} & 1 & 0 \\ a_{obs31} & a_{obs32} & a_{obs33} \end{bmatrix} + \\ &\begin{bmatrix} 0 \\ \theta \\ -(c_1 + c_2 + c_3) \theta - \dot{\theta} \end{bmatrix} + O_{bs}^{-1} L_{bs} y, \quad (42) \end{aligned}$$

where

$$\begin{aligned} a_{obs31} &= -\left( c_1 + c_3 + c_1 c_2 c_3 + \frac{a}{b} (c_1 + c_2 + c_3) \right) L_{bs1} \\ &+ (c_1 + c_2) L_{bs2} - L_{bs3}, \\ a_{obs32} &= -\left( c_1 c_2 + c_1 c_3 + c_2 c_3 + \frac{a}{b} + 2 \right), \\ a_{obs33} &= -(c_1 + c_2 + c_3). \end{aligned}$$

The observer-based backstepping control system is given by.

$$\dot{x} = f(x) + g(x) \hat{u}, \quad (43a)$$

$$\dot{\hat{x}} = f(\hat{x}) + g(\hat{x}) \hat{u} + O_{bs}^{-1} L_{bs} (y - \hat{x}_1). \quad (43b)$$

For any arbitrary initial condition  $x(0) = x_0, \hat{x}(0) = \hat{x}_0$  substituting Eq. (34) in Eq. (43a) yields the closed loop form as

$$\begin{aligned} \dot{x} &= \begin{bmatrix} 0 \\ 0 \\ cb(x_2 - \hat{x}_2) + d(x_3 - \hat{x}_3) \end{bmatrix} + \\ &\begin{bmatrix} x_2 \\ \frac{a}{b} x_1 + x_3 + \theta \\ k_{cl1} \hat{x}_1 + k_{cl2} \hat{x}_2 + k_{cl3} \hat{x}_3 + k_{cl3} \theta - \dot{\theta} \end{bmatrix}. \quad (44) \end{aligned}$$

$$k_{cl1} = c_1 + c_3 + c_1 c_2 c_3 + \frac{a}{b} (c_1 + c_2 + c_3),$$

$$k_{cl2} = c_1 c_2 + c_1 c_3 + c_2 c_3 + \frac{a}{b} + 2,$$

$$k_{cl3} = c_1 + c_2 + c_3.$$

Whereas  $x_2 \rightarrow \hat{x}_2$  and  $x_3 \rightarrow \hat{x}_3$ , the terms  $cb(x_2 - \hat{x}_2) \rightarrow 0$  and  $d(x_3 - \hat{x}_3) \rightarrow 0$ , whereby the above equation reduces to,

$$\dot{X} = \begin{bmatrix} x_2 \\ \frac{a}{b} x_1 + x_3 + \theta \\ k_{cl1} \hat{x}_1 + k_{cl2} \hat{x}_2 + k_{cl3} \hat{x}_3 + k_{cl3} \theta - \dot{\theta} \end{bmatrix}. \quad (45)$$

7. Simulation Results

7.1. Results for the BS control System

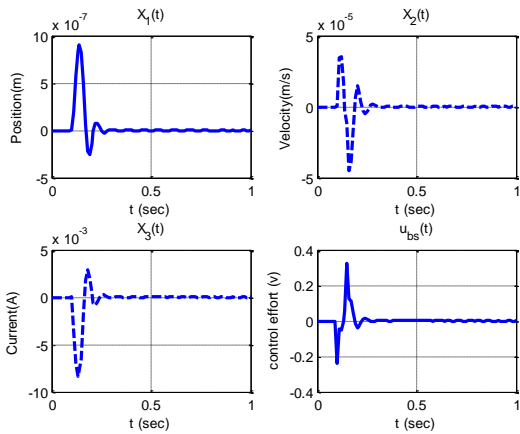


Figure 2. Shows the system response to a disturbance in the rotor position  $c_1 = 200, c_2 = 150, c_3 = 200, x_1(t) \rightarrow 0, u(t) \rightarrow 0$ .

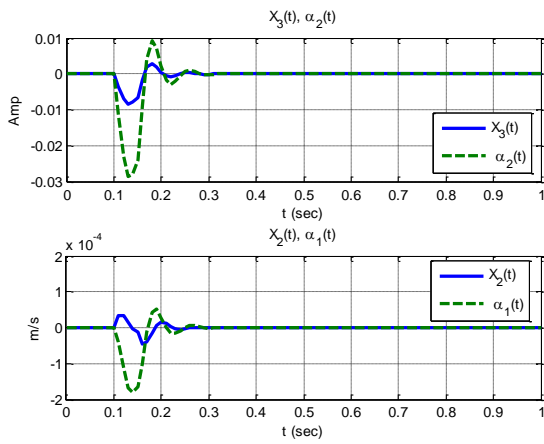


Figure 3. Shows the convergence of the virtual controls to the actual states.  $\alpha_1 \rightarrow x_2(t), \alpha_2 \rightarrow x_3(t)$ .

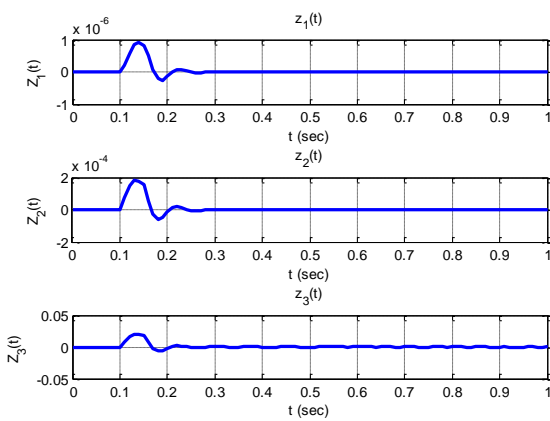


Figure 4. Regulator response  $z_1(t) \rightarrow 0, z_2(t) \rightarrow 0, z_3(t) \rightarrow 0$

7.2. Results for the observer-based BS control System

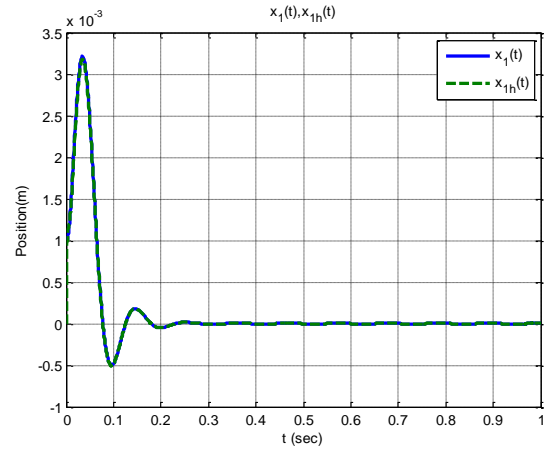


Figure 5. OB-Backstepping regulator with  $c_1 = 100, c_2 = 100, c_3 = 100, x_{1h}(t) \rightarrow x_1(t) \rightarrow 0$

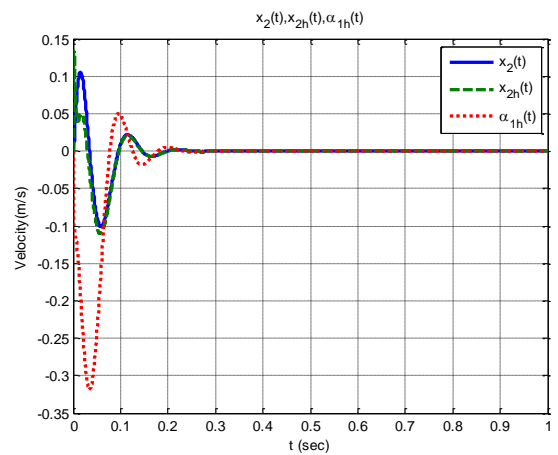


Figure 6. OB-Backstepping regulator with  $c_1 = 100, c_2 = 100, c_3 = 100, \alpha_{1h}(t) \rightarrow x_{2h}(t) \rightarrow x_2(t)$

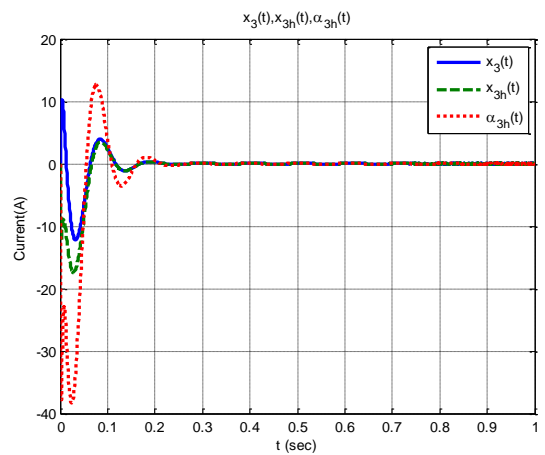


Figure 7. OB-Backstepping regulator with  $c_1 = 100, c_2 = 100, c_3 = 100, \alpha_{2h}(t) \rightarrow x_{3h}(t) \rightarrow x_3(t)$

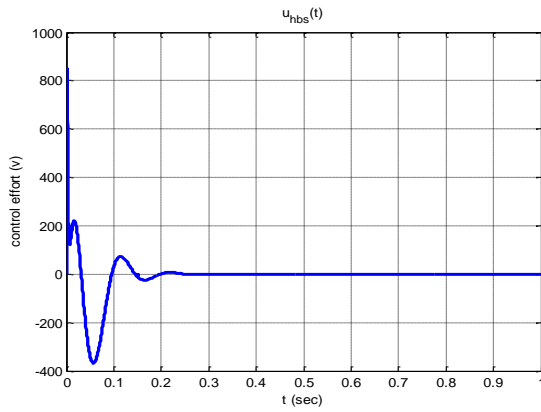


Figure 8. OB-Backstepping regulator with  $c_1 = 100, c_2 = 100, c_3 = 100$ .

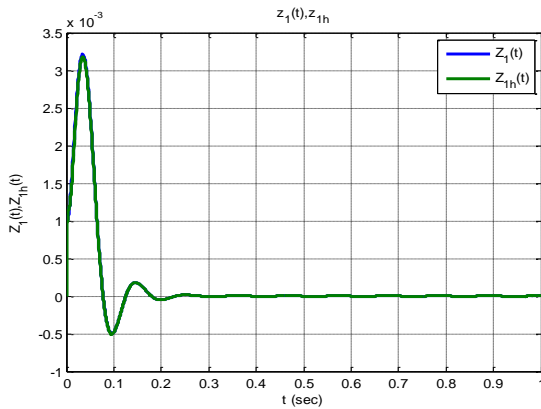


Figure 9. OB-Backstepping regulator with  $c_1 = 100, c_2 = 100, c_3 = 100$ ,  $z_{1h}(t) \rightarrow z_1(t) \rightarrow 0$ .

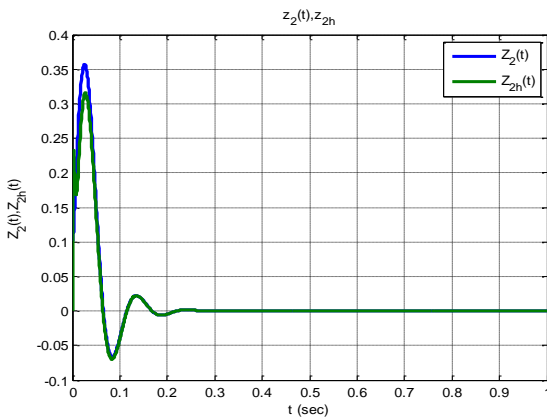


Figure 10. OB-Backstepping regulator with  $c_1 = 100, c_2 = 100, c_3 = 100$ ,  $z_{2h}(t) \rightarrow z_2(t) \rightarrow 0$

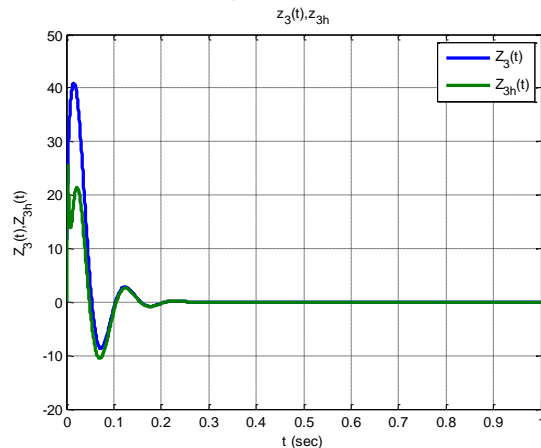


Figure 11. OB-Backstepping regulator with  $c_1 = 100, c_2 = 100, c_3 = 100$ , Showing  $z_{3h}(t) \rightarrow z_3(t) \rightarrow 0$ .

The parameters  $c_1, c_2,$  and  $c_3$  are the backstepping controller tuning parameters, the choice of those values affects the controller performance, they can be tuned to control steady state error, rise time, settling time, overshoot ...etc. They are tuned by guessing and trial and error. The values that gave the best performance for the non-observer-based controller were  $c_1=200, c_2=150, c_3=100$  and the values that gave the best performance for the observer-based controller were  $c_1=c_2=c_3=100$ .

The Active Magnetic Bearing (AMB) was simulated with a pulse disturbance of 4.6 N applied at time 0.1 second. The goal of the control is to ensure the level of clearance between the rotor and the stator of approximately 1mm is not exceeded, meaning that the control should not allow the movement of the rotor to exceed the 1mm and always try to regulate it to the center.

Figures (2) through (4) show the simulation results for the (AMB) system using backstepping control. After applying the disturbance, the control was able to maintain the rotor movement to a maximum of 0.061 mm and converged to its original position in less than 0.2s. Figure 3 shows the convergence of the virtual controls  $\alpha_1$  and  $\alpha_2$  to the corresponding states  $x_2$  and  $x_3$  respectively. The results show the system is asymptotically stable. The errors converge to zero and the rotor position is regulated.

Figures (5) through (11) show the simulation results for the (AMB) system using observer based backstepping control. After applying the disturbance, the control was able to maintain an adequate clearance between the rotor and the stator, a maximum distance of 0.083 mm was measured, and it took the system no more than 0.2s to settle down to its initial position. The system is regulated to its initial position without steady state error. Figure (5) shows the convergence of the estimate of the position  $x_{1h}$  to the true position  $x$ , and the convergence of the Figure (6) shows the convergence of the estimate  $x_{2h}$  of the velocity to the true velocity  $x_2$  and the convergence of the virtual control  $\alpha_1$  to  $x_2$ . Figure (6) shows the convergence of the estimate  $x_{2h}$  of the velocity to the true velocity  $x_2$  and the convergence of the virtual control  $\alpha_1$  to  $x_2$ . Figure (7) shows the convergence of the estimate  $x_{3h}$  of the current to the true current  $x_3$  and the convergence of the virtual control  $\alpha_2$  to  $x_3$ .

### 8. Hypothesis and Limitations

The presented method estimates the system states but does not estimate the disturbance. We added a known value of the disturbance taken from [22] to test the robustness of the controller to disturbances. We are currently investigating the disturbance estimation and considering modifying the observer design to estimate the disturbance as well as the system states. Optimization methods for parameters estimation can be found in [32] and [33].

### 9. Conclusion and Future Work

In this paper, Luenberger-like observer based back stepping control is developed to regulate the rotor position in an AMB system. The asymptotic stability and regulation of the rotor position in the AMB was successfully achieved using the developed method as shown in the simulation results. The Luenberger like observer proved excellent convergence to the true states of the system. The system model was transformed from fourth-order MIMO system into a third order SISO subsystem and a first order SISO subsystem by change of variables before applying the control. Applying the same

method for the fourth order MIMO system is our future investigation. Disturbance estimation was not discussed in this paper. The controller robustness to disturbances was tested by applying a pulse disturbance which is assumed to be known (its value was taken from another paper). Disturbance study and estimation is the subject of our future investigation.

## References

- [1] Lichuan Li, Tadahiko Shinshi, and Akira Shimokohbe, "State Feedback Control for Active Magnetic Bearing Based on Current Change Rate Alone". *IEEE Transactions on Magnetics*, (40) 6 (2004) 3512-3517.
- [2] Parinya Anantachaisilp, Zongli Lin, "Fractional-Order Surge Control of Active Magnetic Bearings Suspended Compressor". *Actuators*, (9) 3 (2020) 75-98.
- [3] B. Polajžer, J. Ritonja, G. Štumberger, D. Dolinar and J.-P. Lecointe, "Decentralized PI/PD position control for active magnetic bearings". *Electrical Engineering*, 89 (2006) 53–59.
- [4] Suraj Gupta, et al, "Closed Loop Control of Active Magnetic Bearing Using PID Controller". *Proc. of International Conference on Computing, Power and Communication Technologies (GUCON)*, Galgotias University, Greater Noida, UP, India (2018) 686-690.
- [5] You, Zhenzhen. "Fault Tolerant Control Method of Power System of Tram Based on PLC". *Jordan Journal of Mechanical and Industrial Engineering*, 15.1 (2021) 133-142.
- [6] Zhang, Qian. "Interference Suppression Control Method for Aircraft Electromechanical Speed Control System". *Jordan Journal of Mechanical and Industrial Engineering* 16.1 (2022) 19-29.
- [7] Rafal Piotr Jastrzebski, Riku Pollanen, "Centralized Optimal Position Control for Active Magnetic Bearings: Comparison with Decentralized Control". *Electrical Engineering*, 91 (2009) 101-114.
- [8] Wojciech Grega, Adam Pilat, "Comparison of Linear Control Methods for an AMB system". *International Journal of Applied Mathematics and Computer Science*, 15.2 (2005) 245-255.
- [9] Li, Jingpu, Pengcheng Sheng, and Kaikai Shao. "Optimization of Clutchless AMT Shift Control Strategy for Electric Vehicles". *Jordan Journal of Mechanical and Industrial Engineering* 14.1 (2020) 109-117.
- [10] Ha-Yong Kim, Chong-Won Lee, "Design and Control of Active Magnetic Bearing System with Lorentz Force-Type Axial Actuator". *Mechatronics*, 16 (2006) 13–20.
- [11] Ladislav Kucera, "Robustness of Self-Sensing Magnetic Bearing". *Proceedings of the Magnetic Bearings Industrial Conference*. 1997. p. 261-270, Alexandria, Virginia, USA.
- [12] Myounggyu D. Noh, Eric H. Maslen, "Self-Sensing Magnetic Bearings Using Parameter Estimation". *IEEE Transactions on Instrumentation and Measurement*, vol. 46, no. 1 (1997) 45-50.
- [13] Yuanping Xu, (Member, IEEE), Quan Shen, Yue Zhang, Jin Zhou, Chaown Jin, "Dynamic Modeling of the Active Magnetic Bearing System Operating in Base Motion Condition". *IEEE Access*, 8 (2020) 166003 - 166013.
- [14] S. Saha, SM. Amr, MU. Nabi, A. Iqbal, "Reduced order modeling and sliding mode control of active magnetic bearing". *IEEE Access*, 7 (2019) 113324-113334.
- [15] GP Ren, Z Chen, HT Zhang, Y Wu, et al, "Design of interval type-2 fuzzy controllers for active magnetic bearing systems". *IEEE/ASME Transactions on Mechatronics*, (2020), 25.5: 2449-2459.
- [16] He, Yingqi. "The Electric Vehicle Torque Adaptive Drive Anti-Skid Control Based on Objective Optimization". *Jordan Journal of Mechanical and Industrial Engineering* 15.1 (2021) 39-49.
- [17] Y Zheng, et al, "Unbalance compensation and automatic balance of active magnetic bearing rotor system by using iterative learning control". *IEEE Access*, 7 (2019) 122613-122625.
- [18] X Yan, et al, "Multi-branch convolutional neural network with generalized shaft orbit for fault diagnosis of active magnetic bearing-rotor system". *Measurement*, 171 (2021) 108778.
- [19] Dongsheng Yang, et al, "State-Constraints Adaptive Backstepping Control for Active Magnetic Bearings with Parameters Nonstationarities and Uncertainties". *IEEE Transactions on Industrial Electronics*, (68) 10 (2020) 9822-9831.
- [20] Van-Nam Giap, Shyh Chour Huang, "Effectiveness of fuzzy sliding mode control boundary layer based on uncertainty and disturbance compensator on suspension active magnetic bearing system". *Measurement and Control*, (53) 5-6 (2020) 934-942.
- [21] Kexiang Li, et al, "Field dynamic balancing for active magnetic bearings supporting rigid rotor shaft based on extended state observer". *Mechanical Systems and Signal Processing*, 158 (2021) 107801.
- [22] Niko Nevaranta, et al, Adaptive MIMO pole placement control for commissioning of a rotor system with active magnetic bearings". *Mechatronics*, 65 (2020) 102313.
- [23] Ali Gerami, Roger Fitro, Carl Knospe, "Improving Disturbance Rejection in Nonlinear Active Magnetic Bearing Systems: Using Lur'e Formulation". *Journal of Dynamic Systems, Measurement, and Control*, (142) 4 (2020) 041007- 041014.
- [24] M. Krstic, P.V. Kokotovic, I. Kanellakopoulos. *Nonlinear and adaptive control design*. Wiley, New York, USA (1995) 29-84.
- [25] H. Khalil. *Nonlinear Systems*, 3rd edition, Upper Saddle River, NJ: Prentice-Hall, New Jersey, USA (2002).
- [26] Silu You, "Adaptive Backstepping Control of Active Magnetic Bearing". *Master's Thesis*, Cleveland State University, USA (2007).
- [27] Richard A. Rarick, "Control of An Active Magnetic Bearing with and without Position Sensing". *Master's Thesis*, Cleveland State University, USA (2007).
- [28] Ababneh M., Salah M., Alwidyan K. "Linearization of nonlinear dynamical systems: A comparative study". *Jordan Journal of Mechanical and Industrial Engineering*, Vol. 5, No. 6 (2011) 567 - 571.
- [29] Khasawneh L., Das M., "Adaptive Steering Angle Controller for Autonomous Vehicles in the Presence of Parameter Uncertainty and Disturbances". *International journal of automotive technology*, Vol. 23 No. 5 (2022), 1313–1321.
- [30] Khasawneh L. and Das M., "Lateral Trajectory Tracking Control using Backstepping Method for Autonomous Vehicles," 2021 IEEE International Midwest Symposium on Circuits and Systems (MWSCAS), Lansing, MI, USA, 2021, 1013-1016.
- [31] Salam Mahmoud, Mohammad Merei, "Adaptive Backstepping Position Controller for PMSM Drive with Uncertainties of Mechanical Parameters". *Jordan Journal of Mechanical and Industrial Engineering*, Vol. 14, No. 2 (2020) 249 - 255.
- [32] Zhang, Jun, Shuli Sun, and Hoang Anh Tuan. "Optimization Design and Analysis of Rotary Indexing Mechanism of Tool Magazine in Machining Center". *Jordan Journal of Mechanical and Industrial Engineering* 14.1 (2020).
- [33] Hayajneh, Mohammed T., Montasser S. Tahat, and Joachim Bluhm. "A study of the effects of machining parameters on the surface roughness in the end-milling process". *Jordan Journal of Mechanical and Industrial Engineering* 1.1 (2007) 1-5.